Fast Physical Optics Simulation of the Dual-Reflector Submillimetre-Wave Telescope on the ESA PLANCK Surveyor

Vladimir Yurchenko, John Anthony Murphy, Jean-Michel Lamarre

Abstract **– We present physical optics simulations of the dual-reflector submillimetre-wave telescope on the ESA PLANCK surveyor. The telescope is of a non-conventional Gregorian configuration, with two ellipsoidal reflectors providing a very large field of view at the focal plane where the array of 76 horn antennas feeding low-temperature detectors is located. We analyse defocusing effects of the system, polarization characteristics of the telescope, and the optical performance of high-frequency channels based on special multi-mode horns operating at 545 and 857 GHz.**

I. INTRODUCTION

ESA PLANCK surveyor is being designed for imaging the temperature anisotropies and polarization characteristics of the cosmic microwave background over the whole sky with unprecedented sensitivity, accuracy and angular resolution using nine frequency channels ranging between 25 and 1000 GHz [1].

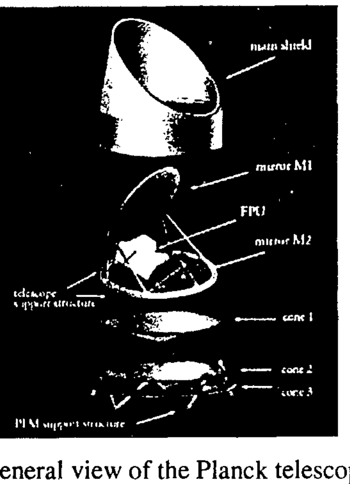

Fig. 1: A general view of the Planck telescope

To achieve this goal, the PLANCK surveyor utilizes a special dual-reflector submillimetre-wave telescope of a non-conventional Gregorian configuration. Both the design and simulation of such a telescope are extremely challenging. Firstly, the telescope is electrically large, the primary mirror having a projected aperture diameter of D=1500 mm while the minimal wavelength involved is only about λ=0.3 mm (i.e., D/λ=5000). Secondly, it is an axially asymmetric system that consists of two essentially defocused ellipsoidal reflectors providing a very large field of view at the focal plane where the array of 76 horn antennas feeding low-temperature detectors is located. To add to the complexity, 14 channels operating at the highest frequencies of 545 and 857 GHz, are based on the multi-mode horns [2] designed for receiving maximum microwave power within the required angular resolution of 5 arcminutes on the sky. Polarization characteristics of the microwave background should be measured in different channels as well.

Among various simulation techniques appropriate for such a design, physical optics is the most adequate one for the given problem [3, 4]. However, conventional implementations of the technique are unacceptably slow. Our implementation overcomes the limitations of a generic approach for large multi-reflector systems and can perform typical simulations of the telescope in the order of minutes.

II. GEOMETRY OF THE TELESCOPE AND DETECTOR UNIT

A general view of the Planck telescope is shown in Fig.1 and a view of the entrance horns of High-Frequency Instrument (HFI), as seen from the telescope, is given in Fig.2 [5].

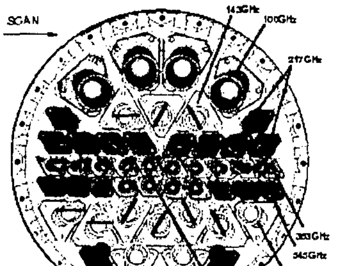

Fig. 2: A view of the entrance horns of HFI

In this paper, we consider power patterns, polarization characteristics and defocusing effects of two beams that correspond to the horns H-143-4 (f =143 GHz) and H-545-1 (f =545 GHz), the ones on the extreme left in the second and in the fourth rows from the bottom in Fig.2 (notations in Fig.2 and some parameters referenced in [1] are out of date).

Vladimir Yurchenko is with the Institute of Radiophysics and Electronics, National Academy of Sciences of Ukraine, 12 Proskura St., Kharkiv, 61085, Ukraine
Vladimir Yurchenko is also with the National University of Ireland, Maynooth, Co. Kildare, Ireland
John Anthony Murphy is with the National University of Ireland, Maynooth, Co. Kildare, Ireland
Jean-Michel Lamarre is with the Institut d'Astrophysique Spatiale, Universite de Paris XI, bat.121, 91405, Orsay Cedex, France

H-143-4 is a Gaussian horn with the electric field at the aperture being linearly polarized and given by the formula

$$\vec{E}(r) = E_0 \exp(-r^2 / w_0^2)\, \vec{e}_0 \qquad (1)$$

where r is the radial coordinate, $w_0 = 3.289$ mm is the half-waist of the beam, $a = 5$ mm is the aperture radius and $\vec{e}_0$ is the polarization vector. H-545-1 is a multi-mode conical horn, with the electric field at the aperture given by the set of six modes ($m = 1..6$) defined as follows

$$\vec{E}_m(r) = E_{0m}\, J_n(p_m r / a) \exp(iqr^2)\, \vec{e}_m(\varphi) \qquad (2)$$

where $J_n(.)$ is the Bessel function, $n = 0, 1, 2$ when $m = 1$ or 6, 2 or 3, and 4 or 5, respectively, $p_1 = 2.405$, $p_2 = p_3 = 3.831$, $p_4 = p_5 = 5.136$, $p_6 = 5.520$, $q = \pi / \lambda L$, $L = 28$ mm is the length of the horn, $a = 4.1$ mm is the aperture radius, and $\vec{e}_m(\varphi)$ is the polarization vector depending on the azimuthal angle, $\vec{e}_{1,6} = \hat{j}$, $\vec{e}_{2,3} = \pm\sin(\varphi)\hat{i} + \cos(\varphi)\hat{j}$, and $\vec{e}_{4,5} = \sin(2\varphi)\hat{i} \pm \cos(2\varphi)\hat{j}$. Amplitudes E_0 and E_{0m} in (1) and (2) are normilized so that each mode has the total power $P = 1$. Horn positions and orientations are specified with respect to the reference detector plane P defined as a plane normal to the chief

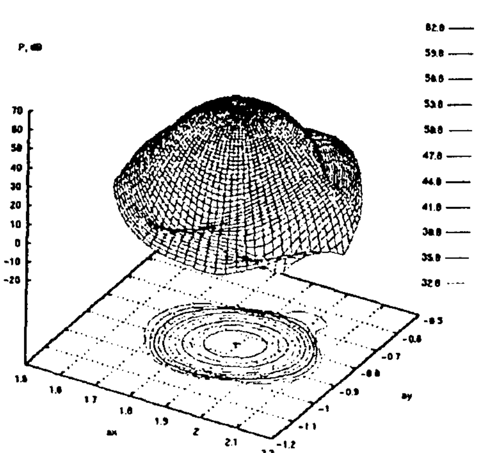

Fig. 3: Power pattern of the beam H-143-4

ray at the (0,0) point that is the paraxial focus of the telescope. When studying defocusing effects, we have the horn axis fixed. The geometrical focus of the horn, F, is specified by the refocus parameter R_F defined as a distance from the plane P to the point F measured along the horn axis, with $R_F > 0$ when moving towards the secondary mirror. Optimum 'geometrical' values of R_F have been provided as a result of the previous design performed with the ray tracing software. For the horns H-143-4 and H-545-1, they are $R_F = 10.5$ mm and $R_F = 5.526$ mm, respectively.

III. Beam from the Gaussian Horn H-143-4

Fig.1 shows the power pattern of the telescope beam from the Gaussian horn H-143-4 as projected on the plane normal to the telescope line-of-sight at (0, 0) point (α_x and α_y are the horizontal and vertical axes on the plane, respectively, measured in degrees). The beam is perfectly shaped down to –30 dB below the maximum, with the beam width being about 8 arcmin at –3 dB.

The polarization of the beam is, generally, elliptical except at the very axis where it remains linear. In order to achieve the required orientation of the polarization pattern in the sky, we should orient the polarization

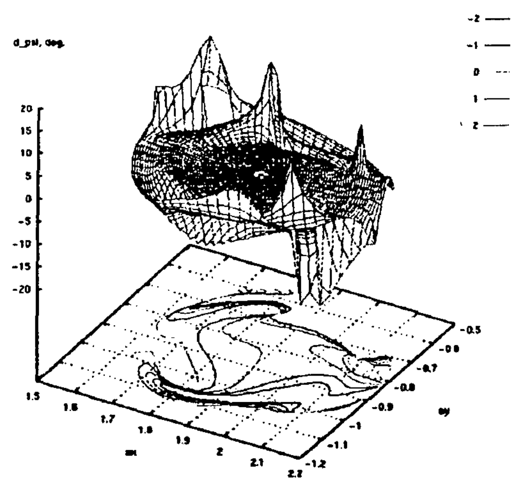

Fig. 4: Deviation of the major axis of polarization ellipse from the local meridian as a function of the observation point within the beam

vector $\vec{e}_0$ properly on the horn aperture. For immediate comparison of polarizations measured by different horns when scanning through the sky, we should use easily aligned directions in the sky as equivalent reference polarization axes for different beams. Such directions are the meridians in the spherical frame of the telescope, with the telescope spin axis being the pole (the meridians define local verticals at various observation points). Also, we should properly define the reference axis for polarization vectors $\vec{e}_0$ of differently tilted horns. We define the reference axis as the direction of $\vec{e}_0$ in the aperture plane that is projected on the vertical axis in the detector plane P. Orientation of $\vec{e}_0$ is specified by the angle φ_e in the aperture plane measured from this reference clockwise when looking from the horn to the secondary mirror.

Using these definitions, we find that the beam from the horn H-143-4 is vertically polarized on the axis (the electric field is directed along the meridian) if the horn polarization vector $\vec{e}_0$ is specified by the angle $\varphi_e = 3.04$ deg.

The deviation of the major axis of the polarization ellipse from the local meridian as a function of the observation point within the beam is shown in Fig.4.

When the polarization is properly adjusted, the cross-polarized component of the field measured with respect to the given direction is minimized. For example, in the case of the vertical polarization discussed above, the power pattern of the cross-polarized component measured as the horizontal component of the electric field, is shown

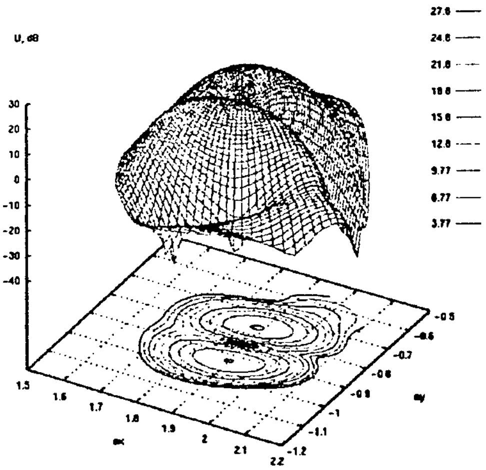

Fig. 5: Power pattern of cross-polarized (horizontal) component of the vertically polarized beam from the Gaussian horn H-143-4

in Fig. 5. It resembles very much the power pattern of the minor axes of polarization ellipses, being only somewhat greater in magnitude at the points where the polarization ellipse is more tilted with respect to the local meridian.
Observing Figs. 3 and 5, we can see that the cross-polarizied component in this case is about –35 dB below the co-polarized one that constitutes the main power of the beam. For comparison, if the polarization vector $\vec{e}_0$ is not properly adjusted ($\varphi_e = 0$), the cross-polarized component is 10 dB greater than possible minimum.

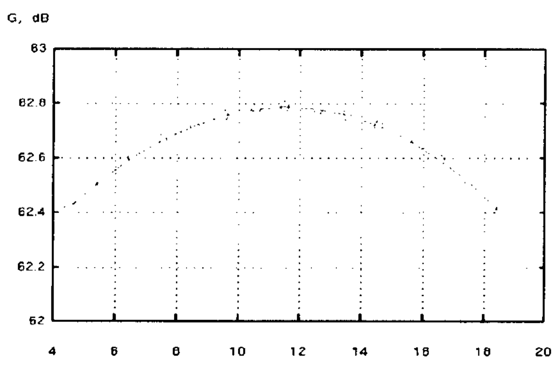

Fig. 6: Defocusing effect of the horn H-143-4

Finally, Fig. 6 shows the defocusing effect of the horn on the gain function G defined as

$$G = 10\log_{10}(4\pi P(0)/P) \qquad (3)$$

where $P(0)$ is the power flux on the beam axis and $P = 1$ is the total power of the beam. The position of the horn is specified by the refocus parameter R_A similar to R_F but measured to the centre of the horn aperture. For the Gaussian horn with the plane phase front at the aperture, the optimum value of R_A is expected to be about R_F. Indeed, Fig. 6 shows that the optimum position is only 1 mm = 0.5λ ahead of the geometrical focus R_F, and the variation of G is sufficiently small, being only 0.4 dB within the range of ± 7 mm = $\pm 3.5\lambda$ around the optimum point.

IV. BEAM FROM THE MULTI-MODE HORN H-545-1

Multi-mode horns are designed for receiving maximum microwave power within the required angular resolution consistent with the requirements on the beam taper at the secondary mirror at the level of –30 dB, with the aspect angle of 20 degrees. These are rather restrictive and contradictory requirements resulting in a rather big aperture area of the corrugated conical horns.
Since the phase front of the horn aperture field is convex, the effective focal centre is located inside the horn at the distance R_C from the aperture. For the horn H-545-1, assuming the shape of the beam approximately Gaussian, R_C is estimated as $R_C = 25.8$ mm. It is expected that the horn is properly focused if the aperture refocus parameter R_A is $R_A = R_F + R_C = 31.3$ mm. In this case, since the total field of the horn is quite uniform within the aperture and rapidly decays outside the horn, one should expect the far-field pattern of the telescope beam to be just a map of the aperture field, with the beam being perfectly shaped. The full beam width is estimated $W = 2Ma = 14$ arcmin where $M = 1.72$ arcmin/mm

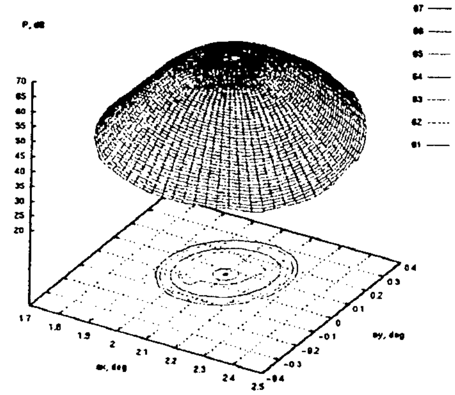

Fig. 7: Power pattern of the multi-mode horn H-545-1 placed 'in-focus' ($R_A = 31.3$ mm)

is the magnification of the telescope and $a = 4.1$ mm is the horn aperture radius.
The power pattern of the telescope beam computed in this case is shown in Fig. 7. The beam is quite symmetrical, well shaped and has a flat top but it is too wide compared to the requirements. The edge of the flat top is about –3 dB below the maximum, and the beam width at the edge is approximately 17 arcmin that is quite close to the estimate above but more than three times greater compared to the required resolution of 5 arcmin.

In order to find the optimum position of the horn, we studied defocusing effect in a wide range of the refocusing parameter R_A, Fig. 8.

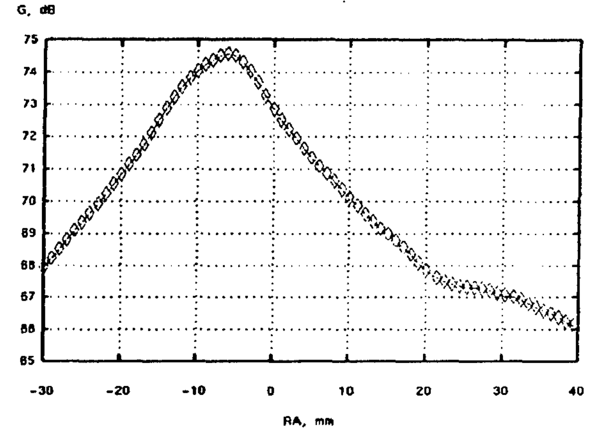

Fig. 8: Defocusing effect of the horn H-545-1

In terms of the gain G defined in (3) where $P(0)$ is the flux along the beam axis of the total power of all the modes in both polarizations and $P = 1$ is the power of a single mode, the maximum gain is achieved when $R_A = -6$ mm.

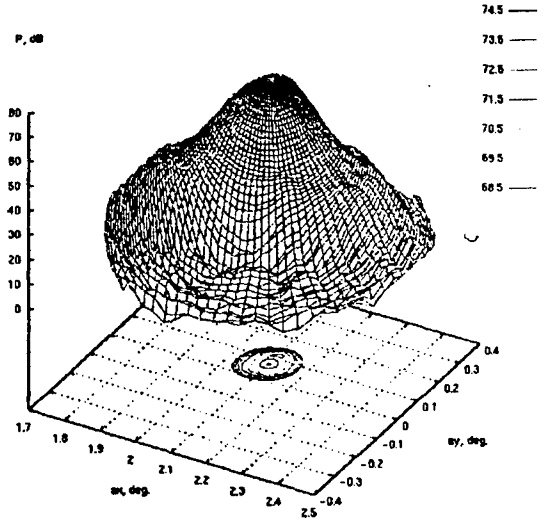

Fig. 9: Power pattern of the horn H-545-1 placed at the position of $R_A = -6$ mm providing the maximum gain $G = 74.5$ dB

The beam pattern computed in this case is shown in Fig. 9. As one can see, the total power of the beam is concentrated in a much smaller area resulting in a significant increase in the gain G. The beam is still slightly flat topped, although not so perfect, being of elliptical shape. The effective width of the beam at the edge of the flat top (at –3 dB) varies from $W_{\min} = 6$ arcmin to $W_{\max} = 7.5$ arcmin that is just slightly greater than the desired angular resolution of the telescope at the given frequency. Power patterns of different modes composing the beam are shown in Fig. 10.

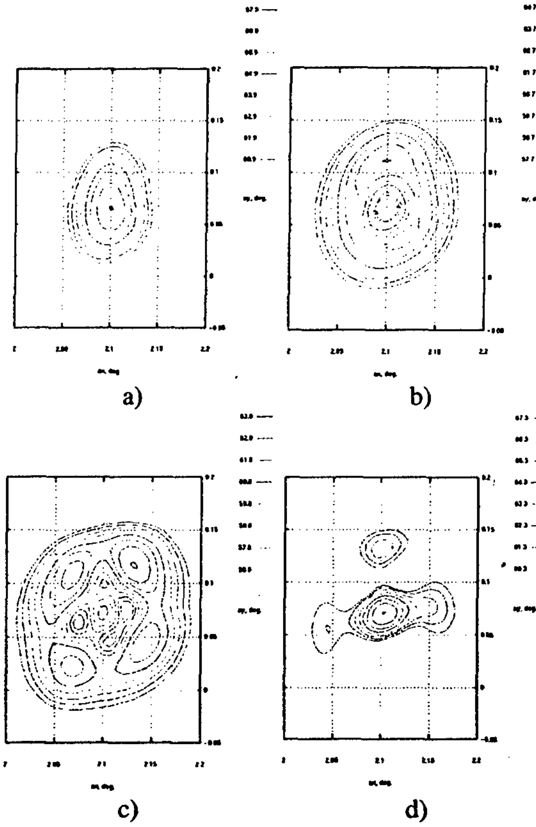

Fig. 10: Power patterns of different modes: (a) m=1; (b) m=2,3; (c) m=4,5; (d) m=6

V. Conclusion

Fast physical optics simulator has been developed for the analysis of the dual-reflector submillimetre-wave telescope on the ESA Planck Surveyor. Study of the power patterns, polarization, defocusing effects and modal structure of the telescope beams from both the Gaussian and molti-mode horns operating at 143 and 545 GHz, respectively, has been performed.

Acknowledgement

The authors are grateful to Yuying Longval for providing updated positions and aiming angles of the high-frequency horns. V.Y. and J.A.M. would like to acknowledge the support of Enterprise Ireland.

References

1. http://astro.estec.esa.nl/Planck
2. R. Colgan, J. A. Murphy, B. Maffei, C. O'Sullivan, R. Wylde, P. Ade, "Modelling Few-Moded Horns for Far-IR Space Applications", to appear in Eleventh Int. Symp. on Space Terahertz Technology, 2000
3. L. Diaz, T. Milligan, Antenna Engineering Using Physical Optics: Practical CAD Techniques and Software, Artech House, London, 1996
4. C. Scott, Modern Methods of Reflector Antenna Analysis and Design, Artech House, London, 1990
5. http://astro.estec.esa.nl/Planck/pictures/pictures_top.html